Theoretical study of all-optical NRZ to RZ format conversion with tunable pulse width based on XPM in a silicon waveguide

ZHANG Bo-lin(张博琳) **and SONG Mu-ping**(宋牟平)*

Department of Information Science and Electronic Engineering, Zhejiang University, Hangzhou 310027, China

(Received 30 August 2011)

An all-optical format conversion from non-return-to-zero (NRZ) to return-to-zero (RZ) is presented based on cross-phase modulation (XPM) in a silicon waveguide with a detuned optical bandpass filter (OBPF). The simulation results show that the tunable bandwidth of the OBPF leads to RZ signals with tunable pulse width. The conversion efficiency (CE) and the pattern effect of the RZ signal are attributed to the parameters of the pump pulse and the OBPF. The converted RZ signal exhibits lower timing jitter than the NRZ signal.

Document code: A **Article ID:** 1673-1905(2012)01-0056-4

DOI 10.1007/s11801-012-1114-3

All-optical format conversion is a key technique in the future optical communication system. Much effort has been made on all-optical non-return-to-zero (NRZ) to return-to-zero (RZ) format conversion, which is mainly based on cross-phase modulation (XPM) or four-wave mixing (FWM) in nonlinear devices, for example, semiconductor optical amplifier (SOA)[1,2]. However, SOA is a kind of active device which requires current injection electronics and a heat-sink platform. To overcome this problem, nonlinear fiber[3] seems to be a solution, but the low nonlinear coefficient results in a long interaction length. Silicon waveguide, which is a passive device with a high nonlinear coefficient, is suitable for all-optical format conversion[4].

Here, an all-optical format conversion from NRZ to RZ is investigated in a silicon waveguide with a detuned optical bandpass filter (OBPF). It is shown that the quality of the converted RZ signal is influenced by the properties of the pump and the OBPF, respectively. What is more, the RZ signal exhibits lower timing jitter than the NRZ signal.

A strip silicon waveguide is shown in Fig.1 with the light propagating along the $[1\bar{1}0]$ direction. The silicon oxide layer ensures the optical isolation from the high-index silicon substrate, and reduces the losses due to leakage modes. As silicon is a centrosymmetric bulk medium, it has negligible second-order optical nonlinearity and relatively large third-order nonlinearity[5]. High silicon-air index-contrast silicon waveguide, which has a relatively high nonlinear coefficient, with a Kerr coefficient about 100 times and a Raman gain coefficient about 1000 times larger than those of nonlinear fiber, has been considered as a building block of on-chip nonlinear signal processing devices.

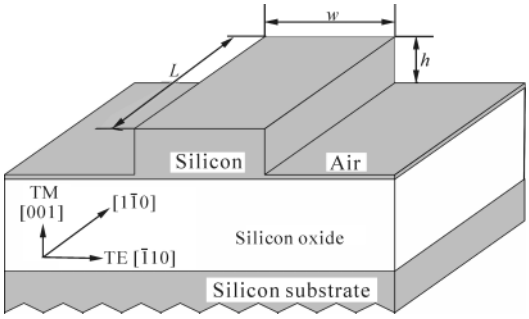

Fig.1 Schematic diagram of strip silicon waveguide structure

A pump wave and a probe wave with the same polarization are launched into the silicon waveguide. Two-photon absorption (TPA) and free-carrier absorption (FCA) can not be neglected when the pump is at high peak power. Taking self-phase modulation (SPM) and XPM into account together with TPA and FCA and designating z as the linear coordinate along the waveguide, we can describe the propagation of the inputs as the following nonlinear Eq.[6]:

* E-mail: songmp@zju.edu.cn

$$\frac{\partial A_{\mathrm{p}}}{\partial z}=-\frac{\alpha}{2}A_{\mathrm{p}}-\mathrm{i}\frac{\beta_2}{2}\frac{\partial^2 A_{\mathrm{p}}}{\partial t^2}+\mathrm{i}\beta^{\mathrm{f}}A_{\mathrm{p}}+(\mathrm{i}\gamma_{\mathrm{p}}-\frac{\beta_{\mathrm{TPA}}}{2A_{\mathrm{eff}}})(|A_{\mathrm{p}}|^2+2|A_{\mathrm{s}}|^2)A_{\mathrm{p}}, \quad (1)$$

$$\frac{\partial A_{\mathrm{s}}}{\partial z}=-\frac{\alpha}{2}A_{\mathrm{s}}-\mathrm{i}\frac{\beta_2}{2}\frac{\partial^2 A_{\mathrm{s}}}{\partial t^2}+\mathrm{i}\beta^{\mathrm{f}}A_{\mathrm{s}}+(\mathrm{i}\gamma_{\mathrm{s}}-\frac{\beta_{\mathrm{TPA}}}{2A_{\mathrm{eff}}})(|A_{\mathrm{s}}|^2+2|A_{\mathrm{p}}|^2)A_{\mathrm{s}}. \quad (2)$$

In Eqs.(1) and (2) A_{p} and A_{s} represent the slowly varying amplitudes of the pump light and probe light, respectively. α is the propagation loss coefficient, β_2 is the group velocity dispersion coefficient, and β_{TPA} is the nonlinear TPA coefficient. The nonlinear coefficient is defined as $\gamma_i=(n_2\omega_i)/(cA_{\mathrm{eff}})$, where i=p, s, and n_2 and A_{eff} are the nonlinear refractive coefficient and waveguide effective area, respectively. Another parameter β^{f} reflects the effects of free carriers and is expressed as

$$\beta^{\mathrm{f}}=\frac{n_0}{n_{\mathrm{eff}}}[k_0 n_{\mathrm{f}}+\frac{i}{2}\sigma_{\mathrm{f}}], \quad (3)$$

where $n_0=3.48$[7] denotes the refractive index of the material, and $n_{\mathrm{eff}}=2.76$ refers to the effective refractive index of the silicon waveguide. n_{f} is the free-carrier dispersion (FCD) coefficient, σ_{f} is the FCA coefficient, and both of them are related to the TPA-induced free-carrier density N. σ_{f}, n_{f} and N are governed by the following equations[8,9]:

$$\sigma_{\mathrm{f}}=1.45\times10^{-17}N, \quad (4)$$

$$n_{\mathrm{f}}=-(8.8\times10^{-4}N+8.5N^{0.8})\times10^{-18}, \quad (5)$$

$$\frac{\partial N(z,t)}{\partial t}=\frac{\beta_{\mathrm{TPA}}}{2\hbar\nu_0}\left(|A_{\mathrm{s}}(z,t)|^2+|A_{\mathrm{p}}(z,t)|^2\right)^2-\frac{N(z,t)}{\tau_{\mathrm{c}}}, \quad (6)$$

where τ_{c} is the carrier lifetime. The parameter values used in this letter are listed as follows: α=3.5 dB/cm[5], $\beta_{\mathrm{TPA}}=5\times10^{-12}$ m/W[10], $n_2=8\times10^{-18}$ m^2/W, A_{eff}=0.12 μm^2, τ_{c}=1.5 ns[11].

To investigate the conversion of 10 Gbit/s non-return-to-zero on-off-keying (NRZ-OOK) to return-to-zero on-off-keying (RZ-OOK) in a silicon waveguide, the simulation setup is used as shown in Fig.2(a). In the NRZ-OOK transmitter, a continuous wave at 1540 nm (λ_{s}) is fed into a Mach-Zehnder modulator (MZM) to obtain a 10 mW NRZ signal as the probe, which is driven by a 10 Gbit/s pseudo random binary sequence (PRBS) with a length of 2^8-1. The spectrum of the input NRZ signal is shown in Fig.2(b). The pulsed source generates a 10 GHz periodic pulse train to be the pump at 1553.5 nm (λ_{p}). The average power is 50 mW, the pulse width is 2.7 ps, and the time period is 100 ps. The pump is launched into the silicon waveguide accompanied by the probe after the synchronization of the two input signals by an optical delay line (ODL). With the XPM effect, the output NRZ signal from the silicon waveguide is shown in Fig.2(c). The following OBPF, which is a three-pole band-pass Bessel filter, is used to extract RZ signal. The OBPF central wavelength is 1542 nm and the corresponding wavelength detuning is 2 nm. Then the spectrum of the converted RZ signal as shown in Fig.2(d) is extracted.

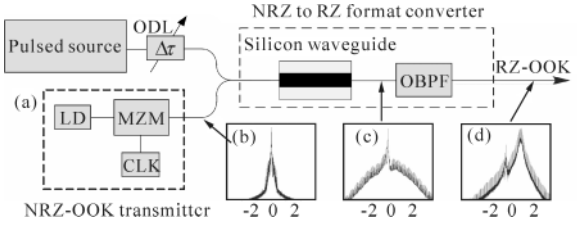

Fig.2(a) Simulation setup to carry out the conversion of 10 Gbit/s NRZ-OOK to RZ-OOK and the spectra of (b) the input NRZ signal, (c) the output NRZ signal from the silicon waveguide and (d) the converted RZ signal

As shown in Fig.3, the pump pulse train is synchronized with the NRZ signal. With the effect of XPM in the silicon waveguide, the frequency chirp in Fig.3 is negative (red shift) at the rising edge of the pump pulse, while positive (blue shift) at the falling edge. These transient induced-frequency shifts are within the pump duration. The OBPF with proper detuning can only transmit the induced-frequency shifted

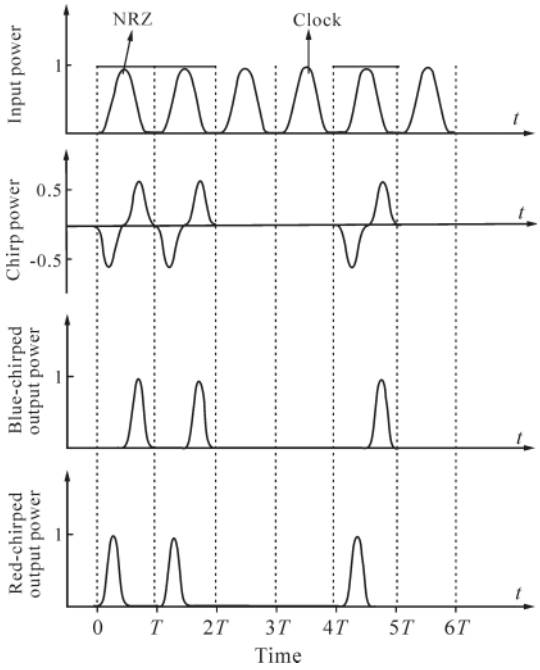

Fig.3 Time domain evolution of pump synchronized with the probe, frequency chirp induced by XPM, RZ from the blue-chirped components and RZ from the red-chirped components

components, and then the RZ signal can be extracted from the broadened spectrum of the NRZ signal (Fig.2). Fig.3 also shows the time domains of RZ from the blue-chirped and the red-chirped components, respectively.

Timing jitter is a major effect which degrades the performance of receiver. To further investigate the retiming performance, the input NRZ signal is distorted by attenuating the power and passing it through an erbium doped fiber amplifier (EDFA) to add the amplified spontaneous emission (ASE). The insets of Fig.4 are the eye diagrams of the NRZ and RZ signals, respectively. With the increase of NRZ noise, namely the decrease of the optical signal noise ratio (OSNR), the corresponding root mean squares (RMSs) of timing jitters of the NRZ and RZ signals both increase as the solid line shown in Fig.4. Because the solid line is below the dash line with the slope of 1, the timing jitter is reduced after the conversion, and the timing jitter reduction increases with the decrease of the input OSNR.

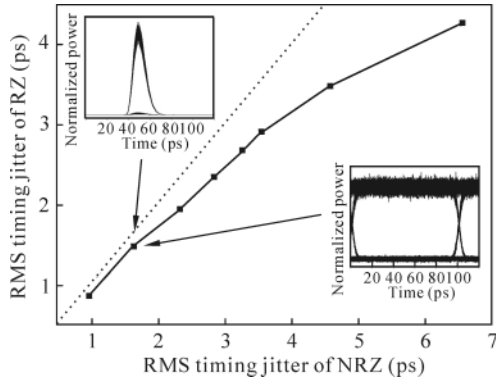

Fig.4 Comparison of RMS timing jitters between the NRZ and RZ signals with a decreasing OSNR

The relationship between the OBPF bandwidth and the RZ pulse width is illustrated in Fig.5, when the OBPF is located in the red sideband (1542 nm) and the blue one (1538 nm) of the broadened spectrum of the NRZ signal. Both curves make it clear that the RZ pulse width is in inverse proportion to the OBPF bandwidth. In addition, the pulse width of the RZ signal is much wider than that of the pump pulse, and the pulse width tunability of red-shift is the same as that of the blue-shift. As we know, the Fourier transform-limited

$$k_{\mathrm{B}} = \sqrt{\frac{2\ln 2}{a}}\sqrt{\frac{2a\ln 2}{\pi}} = \frac{2\ln 2}{\pi} \approx 0.441 \tag{7}$$

is a key parameter for an unchirped Gaussian pulse, where a is Gaussian parameter. From Fig.5 we can calculate the average k_{B} as 0.458, which is close to 0.441. As the OBPF bandwidth changes, tunable-pulse width RZ signal with high quality can be obtained in this way.

Due to the TPA effect, the RZ power reaches the maximum value gradually as displayed in Fig.6. The conversion efficiency (CE) depends on the RZ power, so the curve of CE is similar to that of the RZ power. From the inset, we can see the pattern effect which causes the nonlinear patterning (NLP). NLP is defined as the ratio of the maximum to the minimum peak power of the RZ signal. The value of NLP in Fig.6 decreases at the beginning and then keeps steady as the pump peak power increases. The reason is that the pump peak power contributes to the induced-frequency shift and the range of the XPM-induced spectral broadening. High peak power could keep the original central wavelength of the OBPF (1542 nm) still in the range of the spectral broadening. However, as the peak power decreases, reduced range can render 1542 nm. Consequently, the pump peak power should be set at a relatively large value for the sake of reducing the pattern effect and improving the CE.

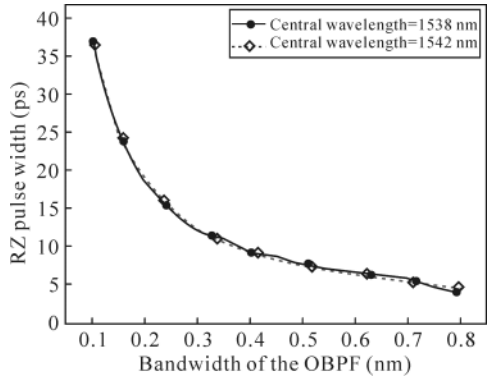

Fig.5 RZ pulse width variation with the bandwidth of the OBPF

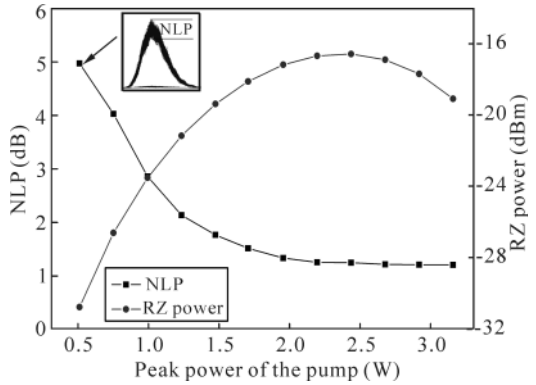

Fig.6 NLP and RZ power variations with the peak power of the pump when the detuning is 2 nm

Fig.7(a) demonstrates that the NLP varies with the pump pulse width when the pump peak power is kept constant. With the pump pulse width increasing, the rising and falling edges of the Gauss pulse get smooth, which lets the frequency chirp

fall off, so the range of the XPM-induced spectral broadening shrinks. In this case, OBPF with lower detuning (< 2 nm) could reduce the pattern effect, which is proved by the pump with pulse width of 7.5 ps as shown in Fig.7(b). The same way can be also applied to low-peak-power condition and the case of the pump with peak power of 0.75 W is shown in Fig.7(b). In conclusion, short pulse train ought to be employed as the pump to enhance the performance of the format converter.

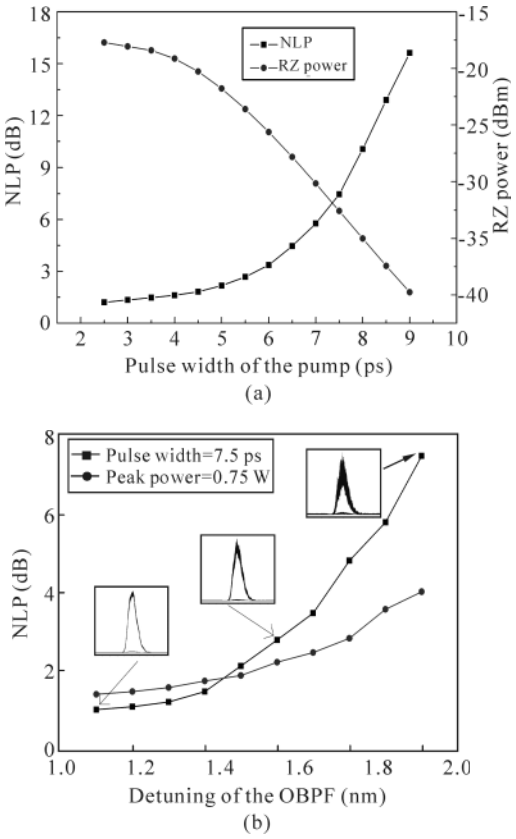

Fig.7(a) NLP and RZ power variations with the pulse width of the pump and (b) NLP variation with the detuning

A silicon waveguide with a detuned OBPF is proposed to achieve an all-optical format conversion from NRZ to RZ based on XPM. By changing the bandwidth of the OBPF, tunable pulse width RZ signal can be achieved with high quality. To improve the CE and reduce the pattern effect of the RZ signal, short or high-peak-power pulse train should be used as the pump. Lower detuning of the OBPF could enhance the quality of the RZ signal with long pulse or low peak power. Moreover, the timing jitter is reduced after the format conversion. The proposed scheme is potential for applications in future optical networks.

References

[1] J. Dong, X. Zhang, F. Wang, Y. Yu and D. Huang, Electron. Lett. **44**, 763 (2008).

[2] Hung Nguyen Tan, Motoharu Matsuura and Napto Kishi, Opt. Express **16**, 19063 (2008).

[3] Akihiro Maruta and Satoru Kitagawa, All-optical Modulation Format Conversion from NRZ-OOK to RZ-multilevel APSK based on Fiber Nonlinearity, IEEE/LEOS Winter Topicals Meeting Series, 207 (2009).

[4] W. Astar, Jeffrey B. Driscoll, Liu Xiaoping, J. I. Dadap, W. M. J. Green, Y. A. Vlasov. G. M. Carter and R. M. Osgood, IEEE J. Sel. Top. Quantum Electron. **16**, 234 (2010).

[5] I-Wei Hsieh, Chen Xiaogang, Jerry I. Dadap, Nicolae C. Panoiu, Richard M. Osgood, Jr. Sharee J. MaNab and Yurii A. Vlasov, Opt. Express **15**, 1135 (2007).

[6] S. Mikroulis, A. Bogris, E. Roditi and D. Syvridis, J. Lightwave Technol. **22**, 2743 (2004).

[7] C. Koos, L. Jacome, C. Poulton, J. Leuthold and W. Freude, Opt. Express **15**, 5976 (2007).

[8] H. K. Tsang, C. S. Wong, T. K. Liang, I. E. Day, S. W. Roberts, A. Horpin, J. Drake and M. Asghari, Appl. Phys. Lett. **80**, 416 (2002).

[9] Ozdal Boyraz, Prakash Koonath, Varum Raghunathan and Bahram Jalali, Opt. Lett. **32**, 2031 (2007).

[10] Yin Lianghong and Govind P. Agrawal, Opt. Lett. **32**, 2031 (2007).

[11] Yin Lianghong, Zhang Jidong, Philippe M. Fauchet and Agrawal P. Govind, Opt. Lett. **34**, 476 (2009).